

Article

**Self-Assembly of CdTe Nanocrystals into Two-Dimensional Nanoarchitectures at the Air–Liquid Interface Induced by Gemini Surfactant of 1,3-Bis(hexadecyldimethylammonium) Propane Dibromide**

Mingxian Liu, Lihua Gan, Yaling Zeng, Zijie Xu, Zhixian Hao, and Longwu Chen

*J. Phys. Chem. C*, **2008**, 112 (17), 6689-6694 • DOI: 10.1021/jp710004t

Downloaded from <http://pubs.acs.org> on December 4, 2008

**More About This Article**

Additional resources and features associated with this article are available within the HTML version:

- Supporting Information
- Access to high resolution figures
- Links to articles and content related to this article
- Copyright permission to reproduce figures and/or text from this article

[View the Full Text HTML](#)



**ACS Publications**  
High quality. High impact.

# Self-Assembly of CdTe Nanocrystals into Two-Dimensional Nanoarchitectures at the Air–Liquid Interface Induced by Gemini Surfactant of 1,3-Bis(hexadecyldimethylammonium) Propane Dibromide

Mingxian Liu, Lihua Gan,\* Yaling Zeng, Zijie Xu, Zhixian Hao, and Longwu Chen

Department of Chemistry, Tongji University, Shanghai 200092, People's Republic of China

Received: October 15, 2007; In Final Form: December 16, 2007

In this paper, we report the self-assembly of CdTe nanocrystals into two-dimensional nanoarchitectures at the air–liquid interface induced by a gemini-type surfactant, 1,3-bis(hexadecyldimethylammonium) propane dibromide (gemini 16–3–16). Used as a subphase, CdTe nanocrystals were synthesized in the aqueous phase with 3-mercaptopropionic acid as a surface modifier. They are monodisperse and have a very narrow size distribution with a mean diameter of around 5 nm. In the surface pressure–area isotherms, the limiting molecular area of gemini 16–3–16 on the aqueous subphase containing CdTe nanocrystals is 0.28 nm<sup>2</sup>/molecule, which is only about one-fourth of that on pure water. This exotic Langmuir behavior implies that there engender particular complexes or organizations at the interface of the gemini surfactant and CdTe nanocrystals. The interfacial monolayer was investigated via transmission electron microscopy and X-ray photoelectron spectroscopy. The results indicate that CdTe nanocrystals in the subphase transferred into the interface and then were incorporated with gemini 16–3–16 monolayer under the electrostatic interaction between the head groups of the gemini molecules and the negatively charged CdTe nanocrystals in subphase. The gemini 16–3–16/CdTe nanocrystal complexes have nanorod-like nanostructures with lengths of 100–300 nm and widths of about 25 nm. A mechanism was proposed to explain the building of the particular 2-D nanoarchitectures at the air–liquid interface, involving the circular domains of gemini 16–3–16, full adsorption of the gemini surfactant on CdTe nanocrystal surfaces and the consequent interfacial self-assembly.

## Introduction

The preparations and properties of nanoparticles of metals, semiconductors, and insulators have attracted great attention in the past several years due to their unique properties different from those of the bulk materials such as optical, electric, magnetic, acoustic, and thermal properties.<sup>1–6</sup> With the further miniaturization of electronic components, optical detectors, chemical and biochemical sensors, and devices, etc., it has become an increasingly important task to fabricate fascinating and functional nanometer-scaled structures and architectures in which it requires immobilization of nanoparticles in different assemblies.<sup>7–10</sup> Assembly of metallic and inorganic nanoparticles into 1-D, 2-D, and 3-D nanostructures is well-known to yield collective physical properties depending on the particle size, spacing, and higher-order structure.<sup>11</sup> Self-assembly is natural basic building principle for producing organized arrays varying from biomolecules to colloid particles with controlled geometrical and physicochemical surface properties. Consequently, in the fabrication of functional nanomaterials and nanodevices, self-assembly method offers substantial advantages over traditional manufacturing approaches.

In 1995, Murray and his co-workers first reported the self-organization of CdSe nanocrystallites into 3-D quantum-dot superlattices.<sup>12</sup> Crystallization was induced by pressure- and temperature-controlled evaporation of a two-solvent mixture containing CdSe nanocrystals. From then on, many 2-D or 3-D self-assembly of nanoparticles were achieved by using different

method in solution.<sup>13–20</sup> The Langmuir and Langmuir–Blodgett (LB) technique provide an effective way for controlling the molecular orientations and packing at the molecular level<sup>21–29</sup> and accordingly offer promising prospects for constructing structurally well-ordered, oriented and organized organic/inorganic and organic/organic complexes with the assistance of amphiphiles.<sup>30–37</sup> However, the self-assembly of monodisperse nanoparticles, especially CdTe nanocrystals, into ordered 2-D or 3-D array at the air–liquid interface, to the best of our knowledge, has been little reported previously.

On the other hand, during the research of interfacial phenomenon, there are considerable interests in gemini-type surfactants that consist of two hydrophobic chains linked by a spacer due to their tunable molecular geometries and unusual physical properties of their aggregates at the air–liquid interface.<sup>38–42</sup> For instance, Zhou et al. reported an unusual spontaneous crystallization of gemini surfactant with a rigid spacer at the air–water interface through the  $\pi$ – $\pi$  stacking interaction of benzene rings.<sup>42</sup> Liu et al. found the supramolecular chirality of the TPPS–gemini system at the interface, although both TPPS and gemini surfactant are achiral.<sup>41</sup>

In this paper, we report a novel approach to assemble CdTe nanocrystals into 2-D nanostructures at the air–liquid interface rather than in solution, which were induced by a cationic gemini surfactant, 1,3-bis(hexadecyldimethylammonium) propane dibromide. By control of the surface pressure of the gemini surfactant monolayer on the aqueous phase containing CdTe nanocrystals, the negatively charged CdTe nanocrystals could transfer from subphase into the gemini surfactant monolayer

\* To whom correspondence should be addressed. E-mail: ganlh@tongji.edu.cn.

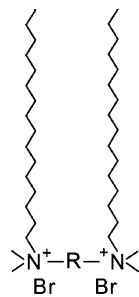


**Figure 1.** The chemical structure of gemini 16-3-16 ( $R = \text{CH}_2\text{CH}_2\text{-CH}_2$ ).

under electrostatic interaction, forming nanorod-like CdTe nanocrystal/gemini surfactant nanocomplexes.

### Experimental Section

Cationic gemini surfactant of 1,3-bis(hexadecyldimethylammonium) propane dibromide ( $(\text{C}_3\text{H}_6\text{-}\alpha,\omega\text{-(C}_{16}\text{H}_{33}\text{N}^+(\text{CH}_3)_2\text{-Br}^-)_2$ , hereafter abbreviated as gemini 16-3-16, molecular structure shown as Figure 1, 99%), was provided by Professor Honglai Liu (East China University of Science and Technology). 3-Mercaptopropionic acid (MPA) was purchased from Aldrich. All other reagents used in this work are analytic reagents purchased from China Medicine (Group) Shanghai Chemical Reagent Corporation. Ultrapure water ( $18.2 \text{ M}\Omega \text{ cm}^{-1}$ ) was used to prepare subphase solutions.

CdTe nanocrystals were synthesized in aqueous phase using MPA as stabilizer according to the method described in ref 43. The prepared CdTe nanocrystal hydrosols were diluted to  $1.0 \times 10^{-5} \text{ mol/L}$  and were used as a subphase of the Langmuir layer. Microdrops of gemini 16-3-16 solution (dissolved in chloroform at a concentration of  $1.0 \times 10^{-4} \text{ mol/L}$ ) were spread evenly on the subphase. Thirty minutes after spreading the sample at the air-liquid interface, the barrier was compressed at a constant speed of 5 mm/min, which was performed on a Finland KSV2000 LB Minitrough operated at room temperature. Contrastively, gemini 16-3-16 was also spread on pure water. The surface pressure vs the specific area isotherms ( $\pi$ - $A$  isotherms) of gemini 16-3-16 on pure water and CdTe nanocrystal hydrosols were also recorded with the KSV LB system.

UV-visible absorption spectrum and photoluminescence spectrum of CdTe nanocrystal hydrosols were measured at room temperature with an Agilent 8453 spectrometer (Agilent) and a LS55 spectrometer (Perkin-Elmer), respectively. Composite monolayer of gemini 16-3-16 and CdTe nanocrystals was obtained by controlling the surface pressure. The monolayer was deposited onto copper grids and quartz substrate, respectively; transmission electron microscopy (TEM, JEM-1230, JEOL) and X-ray photoelectron spectroscopy (XPS, PHI-5400, Perkin-Elmer) were employed to characterize the morphologies and components of the nanocomplexes.

### Results and Discussion

The synthetic CdTe nanocrystals are monodisperse with uniform size distribution of a mean diameter equal to 5 nm, as shown in Figure 2. The CdTe nanocrystal individual has a basically spherical form. CdTe nanocrystals coated with mercapto groups have negatively charged surface, and their surface potential is  $-21.37 \text{ mV}$ , measured by a JS95G+ microelectrophoresis apparatus (Shanghai Zhongchen Digital Technology Apparatus Co. Ltd., China). Therefore, charges on the surface of CdTe nanocrystals and consequent electrostatic interaction

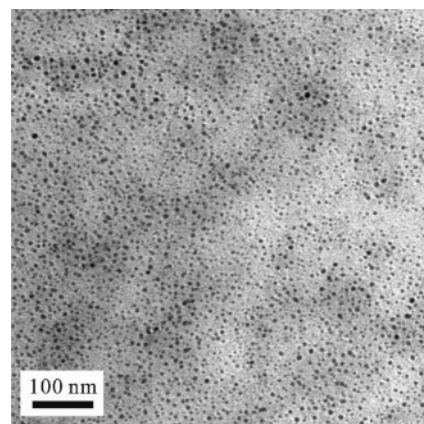


**Figure 2.** TEM image of CdTe nanocrystals.

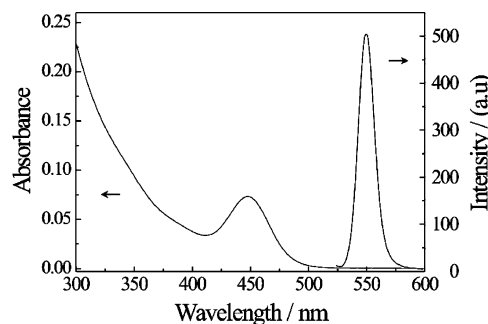


**Figure 3.** UV-vis absorption spectrum and photoluminescence spectrum of CdTe nanocrystal hydrosols.

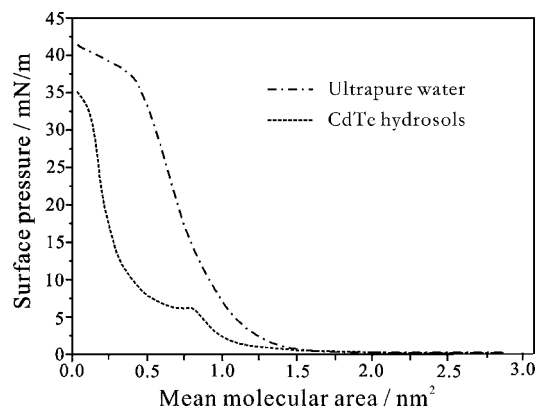


**Figure 4.**  $\pi$ - $A$  isotherms of gemini surfactant 16-3-16 on the subphase of ultrapure water and the aqueous phase containing CdTe nanocrystals.

among CdTe nanocrystals make CdTe nanocrystals disperse evenly throughout the aqueous solution.

The UV-vis absorption and photoluminescence spectra of CdTe nanocrystals are shown in Figure 3. The absorption spectrum of dilute CdTe nanocrystal hydrosols possesses well-resolved electronic transitions, indicating a narrow size distribution of the nanoparticles, being in the size quantization regime.<sup>16</sup> The emission band of CdTe nanocrystals centered at about 550 nm in photoluminescence spectrum (quantum efficiency  $\sim 45\%$  at room temperature) is strong and narrow, also suggesting a narrow size distribution of as-prepared CdTe nanocrystal hydrosols.

Figure 4 shows  $\pi$ - $A$  isotherms of a gemini 16-3-16 monolayer on pure water and the aqueous phase containing monodisperse CdTe nanocrystals, respectively. Both pH values of the subphases were adjusted to 8 by NaOH solution. The  $\pi$ - $A$  isotherm on CdTe nanocrystal hydrosols, compared with



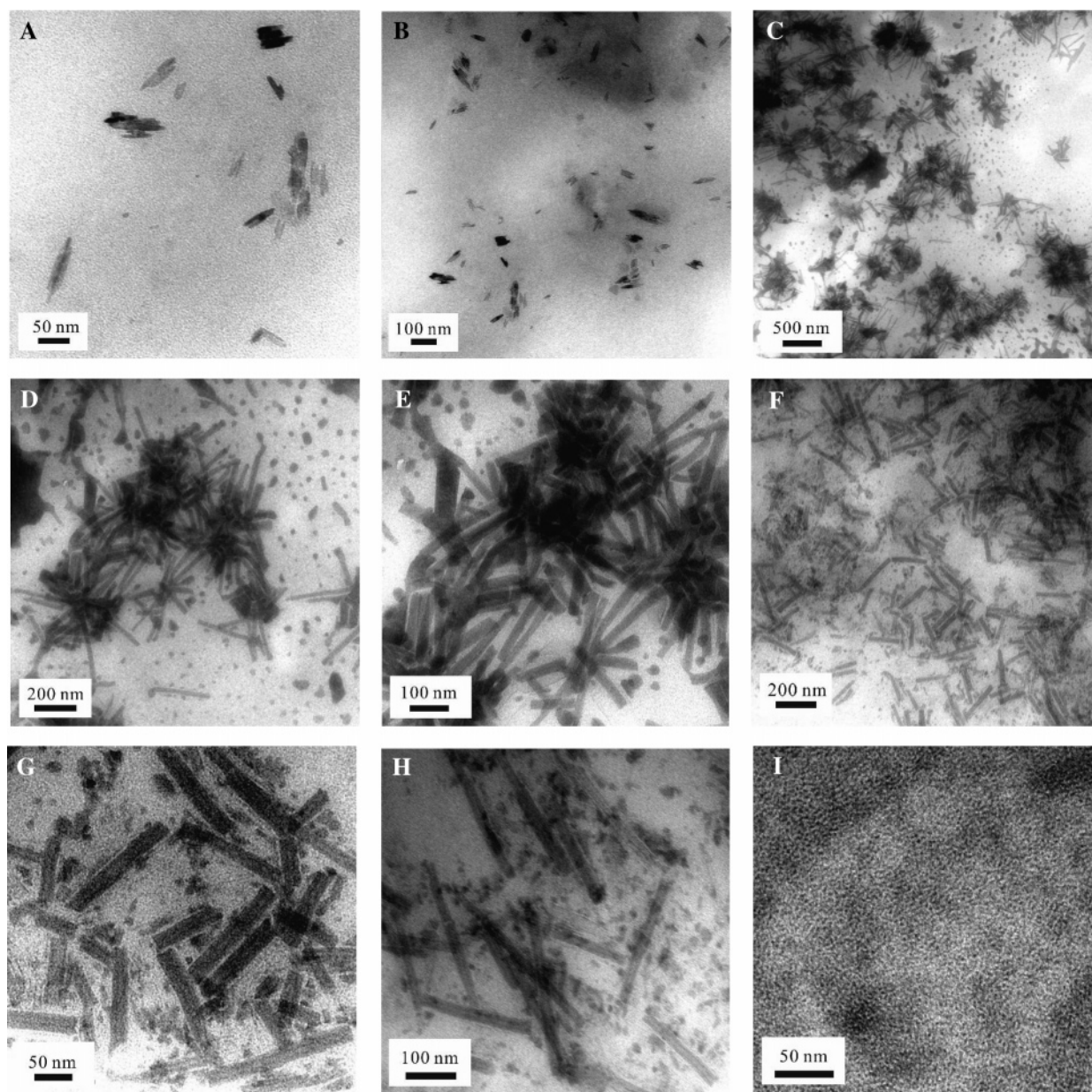


**Figure 5.** TEM images of the composite monolayer of gemini 16-3-16 and CdTe nanocrystals at the air-liquid interface with a surface pressure of 2 (A), 3 (B), 5 (C, D, E), 7 (F, G), 10 (H), and 15 mN/m (I).

that on pure water, exhibits some exotic Langmuir behavior. Besides lower collapse pressure and the plateau region, the most surprising in the  $\pi$ - $A$  isotherms is that the limiting molecular area of gemini 16-3-16 extrapolated by the linear part of the isotherms is only 0.28 nm<sup>2</sup>/molecule. This molecular area is much less than that on pure water (1.05 nm<sup>2</sup>/molecule). In other words, the average molecular area of gemini 16-3-16 on pure water is almost four times bigger than that on CdTe nanocrystal hydrosols. Liu et al. found that the gemini amphiphiles could form stable monolayers at the air-water interface and when the gemini molecules were spread on an aqueous subphase containing opposite-charged molecules or ions, such as an oval decatungstoeuropate (EuW10), a hybrid complex of positively charged gemini amphiphiles and negatively charged EuW10 clusters formed at the air-water interface.<sup>37</sup> Therefore, it is reasonable to think that the gemini 16-3-16 form complexes with CdTe nanocrystals at the interface through the electrostatic interaction. However, the introduction of charged metal ions or nanoparticles into the subphase generally lead to an obvious expanding both in  $\pi$ - $A$  isotherm and mean molecular area for

charged ions or nanoparticles moving into the interfacial monolayer, inhabiting there, and replacing some amphiphiles under the electrostatic interaction between the head groups of amphiphiles and the components in subphase.<sup>22,28-30</sup> Thus the significant reduction of molecular area of gemini 16-3-16 on CdTe hydrosols in the present study implies that some particular complexes or assembly behavior between gemini 16-3-16 and CdTe nanocrystals in the Langmuir layer should be engendered. In addition, the platform occurred at round 5 mN/m in the  $\pi$ - $A$  isotherm obtained on the subphase of CdTe nanocrystal hydrosols also indicates that there create some order aggregates or organizations at this surface pressure, otherwise the surface pressure of gemini 16-3-16 monolayer would increase in the whole  $\pi$ - $A$  isotherm. Besides, it was found in the experiment that the  $\pi$ - $A$  isotherms of the gemini monolayer obtained on the subphase containing CdTe nanocrystals with other pH values, for example, 5.5 and 9.0, show no obvious difference. This should be ascribed to the stability of CdTe nanocrystal hydrosols both in weak acid or alkaline conditions (pH range from 5 to 9), which makes them keep constant luminescence.

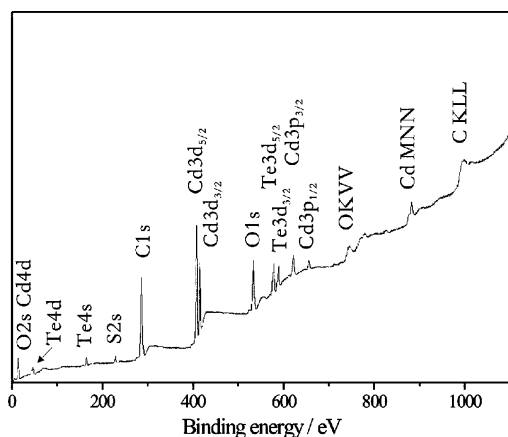


**Figure 6.** XPS spectra of the composite monolayer of gemini surfactant and CdTe nanocrystals.

Figure 5 presents TEM photographs of the gemini 16–3–16 monolayer on the subphase of CdTe nanocrystal hydrosols (pH = 8.0) with different surface pressure. Visible irregular nanopatterns emerged independently at very low surface pressures of 2 mN/m (Figure 5A), and then more nanopatterns formed in the gemini monolayer at 3 mN/m (Figure 5B). What is the most interesting is that the nanopatterns were gradually changed into plenty nanorod-like nanostructures with the surface pressure of 5–7 mN/m, as shown in parts C–G of Figure 5. Figure 5E, the locally magnified result of Figure 5C, shows that the formed nanorod-like nanostructures have lengths of 100–300 nm and widths of about 25 nm. Besides, it is found that the nanostructure of the gemini surfactant/CdTe nanocrystals at higher surface pressure, for example, 10 mN/m, features similar dimensions compared with the complexes obtained from 7 mN/m (Figure 5H). Further compressing the monolayer above 10 mN/m will result in indistinctness of the shapes of the interfacial complexes. The substitute is a whole condensed Langmuir film because the gemini surfactant and CdTe nanocrystals arrange compactly at high surface pressure, as shown in Figure 5I.

From the results of  $\pi$ – $A$  isotherms and TEM investigation, it is obvious that there form some complexes between gemini 16–3–16 molecules and CdTe nanocrystals at the air–liquid interface as a result of the interaction of both. To verify such complexes formed in the monolayer, the XPS spectra of the transferred monolayer were measured. Figure 6 exhibits the XPS spectra of the composite monolayer transferred on quartz substrate at 7 mN/m. CdTe nanocrystals can be confirmed in the monolayer by the binding energies at 11.0 (Cd4d), 44.2 (Te4d), 173.5 (Te4s), 405.0 (Cd3d<sub>5/2</sub>), 412.3 (Cd3d<sub>3/2</sub>), 577.3 (Te3d<sub>5/2</sub>), 587.6 (Te3d<sub>3/2</sub>), 618.2 (Cd3p<sub>3/2</sub>), and 652.5 eV (Cd3p<sub>1/2</sub>). The binding energy at 284.6 eV (C1s) is from the carbon of gemini 16–3–16 in the composite monolayer. The binding energy at 227 eV (S2s) shows the sulfur in MPA coated on the surface of CdTe nanocrystals, while the binding energies at 23.5 eV (O2s) and 531.2 eV (O1s) should be ascribed to either the carboxyls of MPA or the oxidation of the composite monolayer sample. The XPS results, plus the  $\pi$ – $A$  isotherms results indicate that CdTe nanocrystals in the subphase were incorporated into the gemini 16–3–16 monolayer, that is, CdTe nanocrystals transferred into the interface, forming nanorod-like complexes with gemini 16–3–16 under electrostatic interaction. In addition, there also are many unshaped or unintegrated aggregates in the Langmuir layer from TEM images (parts C–E of Figure 5). The aggregates are much bigger than

the CdTe nanocrystal individual in size and accordingly should consist of several CdTe nanocrystals.

The mean area per molecule of gemini 16–3–16 on the CdTe nanocrystal hydrosol subphase is only about a quarter of that on pure water, which is too small to be regarded as the real molecular area of the gemini surfactant. Actually, this Langmuir behavior should be ascribed to the particular nanorod-like self-assembly of CdTe nanocrystals with gemini 16–3–16 at the air–liquid interface. As we have already discussed, if the charged CdTe nanocrystals only pushed away the gemini 16–3–16 (Figure 7B), the limiting molecular area of the gemini molecules should be increased. Therefore, it seems impossible for the configuration of CdTe nanocrystals and the gemini molecules to be the form shown in Figure 7B. In some cases, amphiphiles may form a special aggregation like Figure 7A at the air–liquid interface. For example, Liu et al. found that 2-(heptadecyl)naphtha[2,3]imidazole has such a similar arrangement on pure water.<sup>22</sup> However, this causes only a half reduction of molecular area of amphiphiles.

On the basis of the results from  $\pi$ – $A$  isotherms in Figure 4, we infer that gemini 16–3–16 and CdTe nanocrystals have a particular complexes, shown as Figure 7C. First, the adsorption of the gemini molecules on CdTe nanocrystal surface would be primarily dependent on the negative charges of CdTe nanocrystals. CdTe nanocrystal surfaces take much negative charges, which have strong electrostatic interactions with the ammonium groups of the gemini surfactant. This enables the transferring of CdTe nanocrystals from the subphase into the gemini monolayer. Second, the surface area of CdTe nanocrystal individual is much bigger than that of a single gemini 16–3–16 molecule. As a result, CdTe nanocrystals prefer to absorb the gemini molecules in their surfaces under strong electrostatic interaction other than pushing aside the gemini surfactant. At high surface pressure from which the mean molecule of amphiphiles is extrapolated, we assume the molecular densities of gemini 16–3–16 on pure water and the aqueous phase containing CdTe nanocrystals are  $d_1$  and  $d_2$  (in molecules/nm<sup>2</sup>), respectively. In this case, the mean molecular area of gemini 16–3–16 on pure water ( $A_1$ ) could be calculated as follows

$$A_1 = \frac{1}{d_1} \quad (1)$$

Providing that all of the gemini molecules are adsorbed on the surface of CdTe nanocrystals at high surface pressure, the limiting molecular area of gemini 16–3–16 on CdTe nanocrystal hydrosols ( $A_2$ ) could be given by

$$A_2 = \frac{S_{\text{circle}}}{N} = \frac{S_{\text{circle}}}{d_2 S_{\text{CdTe}}} = \frac{\pi \left(\frac{d}{2}\right)^2}{4\pi \left(\frac{d}{2}\right)^2 d_2} = \frac{1}{4d_2} \quad (2)$$

in which  $S_{\text{circle}}$  is the vertical projective area of CdTe nanocrystal individual at the air–liquid interface (i.e., the actual area the gemini molecules taken at the interface when we calculate the mean molecular area of gemini 16–3–16),  $N$  is the corresponding molecular numbers of gemini 16–3–16 adsorbed on each CdTe nanocrystal surface,  $S_{\text{CdTe}}$  is the surface area of CdTe nanocrystal individual, and  $d$  is the diameter of CdTe nanocrystal.

The inhabitation of gemini 16–3–16 on CdTe nanocrystal surfaces is actually equal to multilayer of gemini molecules at the air–liquid interface, which means great reduction of a virtual amount of gemini molecules when calculating their mean



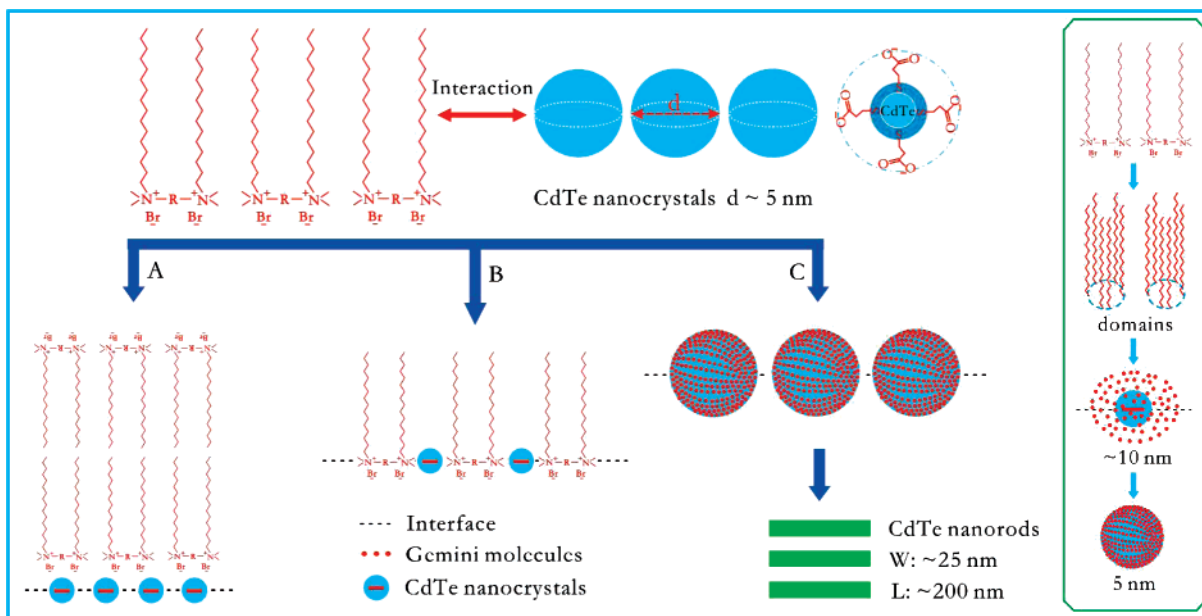


**Figure 7.** Schematic self-assembly behaviors for gemini 16-3-16 and CdTe nanocrystals at the air-liquid interface. The inset shows the probable full-adsorption process of the gemini molecules on the surface of CdTe nanocrystals.

molecular area. At high surface pressure of gemini monolayer, e.g., above  $20 \text{ mN m}^{-1}$  (here the monolayer form a condensed Langmuir film), gemini 16-3-16 arranges compactly both on pure water and on CdTe nanocrystal surface. Therefore, it is reasonable to think that the molecular densities  $d_1$  and  $d_2$  are similar or even equivalent. According to this assumption, eq 2 could be written as

$$A_2 \approx \frac{1}{4d_1} \quad (3)$$

In comparison of eq 1 with eq 3, we immediately have

$$A_1 \approx 4A_2 \quad (4)$$

From eq 4, it can be concluded that the mean molecular area of gemini 16-3-16 obtained from the aqueous phase containing CdTe nanocrystals should be approximately one-fourth of that of gemini 16-3-16 on pure water, matching exactly the results gained from the  $\pi$ - $A$  isotherms. Thus, the calculation results support our presumption that full adsorption model of gemini 16-3-16 on CdTe nanocrystal surfaces at the air-liquid interface. The adsorbed CdTe nanocrystals or gemini 16-3-16/CdTe nanocrystal complexes then aggregated each other by the line tension among the long hydrophobic portions of the gemini molecules to shape nanopatterns at the beginning of compression (as shown in parts A and B of Figure 5). Finally the nanopatterns turn into regular nanorod-like nanostructures by a self-assembly way as the surface pressure increases to 5-7 mN/m. Besides, the nanostructures which consist of CdTe nanocrystals and gemini 16-3-16 should form a monolayer at the air-liquid interface, otherwise the molecular area of the gemini surfactant would be decreased more than three-fourths if interfacial CdTe nanocrystals form multilayer. On the basis of the same reason, the gemini molecules absorbed on the surface of CdTe nanocrystals also should be monolayer.

Why are gemini 16-3-16 molecules apt to be adsorbed fully on CdTe nanocrystal surfaces? We infer that there is something to do with the domains formed by gemini surfactant at the air-liquid interface. Through theoretical calculation, McConnell found various 2-D domain shapes such as circles, rings, ellipses,

etc., at the air-water interface.<sup>44</sup> In the simplest model, the shape of an individual domain of amphiphiles is determined mainly by the competition of the molecular long-range dipolar electrostatic forces  $F_{el}$  and the line tension  $\lambda$  of the boundary between fluid and solid regions<sup>44</sup>

$$F = \lambda p + F_{el} \quad (5)$$

Here  $p$  is the perimeter of the solid domain. The intermolecular electrostatic dipolar repulsions of the hydrophilic groups prefers incompact shapes, whereas the line tension among the long hydrophobic portions favors compact, often isotropic, circular domains.<sup>44-46</sup> The electrostatic dipolar repulsion from the ionic group in gemini 16-3-16 is reduced significantly by the spacer 1,3-propylene ( $\text{C}_3\text{H}_6$ ), which connects the two amphiphilic moieties closely. The intramolecular chain/chain associations of gemini 16-3-16 therefore compete with the electrostatic repulsion of the head groups. Consequently, the interfacial gemini molecules most probably prefer circular domains to irregular ones. Besides, we previously investigated the interfacial interaction between 1, 3-bis(dodecyldimethylammonium) propane dibromide (gemini 12-3-12) and  $\text{Fe}_3\text{O}_4$  nanoparticles and found that gemini 12-3-12 and  $\text{Fe}_3\text{O}_4$  nanoparticles formed hexagonal nanocomplexes at the air-liquid interface with most sides of about 50 nm and some sides of about 30 nm.<sup>47</sup> According to the mechanism proposed, the gemini 12-3-12 formed circular domains with a size of about 10-25 nm. Taking into account the structural similarity between gemini 16-3-16 and gemini 12-3-12, we guess that gemini 16-3-16 molecules also form such circular domains on the aqueous phase containing CdTe nanocrystals with similar size ( $\sim 10$  nm). Interestingly, the circular domain could cover fully the surface of CdTe nanocrystal individual ( $d = 5$  nm) according to the equation

$$\pi\left(\frac{D}{2}\right)^2 = 4\pi\left(\frac{d}{2}\right)^2 \quad (6)$$

in which  $D$  is the diameter of the circular domains. Actually, the domain sizes are probably a little more than 10 nm considering that the molecular density of the gemini surfactant

adsorbed on CdTe nanocrystal surface is most likely higher than that on aqueous phase because of strong electrostatic interaction. The circular domains attracted CdTe nanocrystals transferring from the subphase into the interface, and then they adsorbed on CdTe nanocrystal surfaces (see the insert of Figure 7), and ultimately the complexes are to shape particular 2-D nanoarchitecture by a self-assembly way.

## Conclusions

In conclusion, we have presented a novel nanorod-like nanoarchitecture simply by spreading a gemini 16-3-16 monolayer on the aqueous phase containing CdTe nanocrystals and then controlling the surface pressure. The self-assembled gemini16-3-16/CdTe nanocrystals hybrid nanostructures have lengths of 100–300 nm and widths of around 25 nm. From the three aspects of the circular domains formed by gemini 16-3-16, full adsorption of the gemini surfactant on CdTe nanocrystal surfaces and the consequent interfacial self-assembly, we proposed preliminarily the generation mechanism of these organized nanostructures at the interface. Although the unusual assembly behavior needs further research, the results demonstrated here are meaningful or interesting because they provide the promising prospect for self-organization of nanoparticles toward ordered 2-D and even 3-D architecture with well-defined morphology on the nanometer scale. The air-liquid interface can offer a useful environment for building these novel nanostructures.

**Acknowledgment.** This study was supported by the National Natural Science Foundation of China (Grant Nos. 20473057 and 20673076) and Shanghai Nanotechnology Promotion Center (Grant Nos. 0652nm030 and 0752nm006). The authors also kindly thank Dr. Honglai Liu, professor of East China University of Science and Technology, for the preparation of gemini surfactants of 1,3-bis(hexadecyldimethylammonium) propane dibromide.

## References and Notes

- (1) Murray, C. B.; Norris, D. J.; Bawendi, M. G. *J. Am. Chem. Soc.* **1993**, *115*, 8706.
- (2) Klimov, V. I.; Mikhailovsky, A. A.; Xu, S.; Malko, A.; Hollingsworth, J. A.; Leatherdale, C. A.; Eisler, H.-J.; Bawendiz, M. G. *Science* **2000**, *290*, 314.
- (3) Peng, X.; Manna, U.; Yang, W.; Wickham, J.; Scher, E.; Kadavanch, A.; Allvisatos, A. P. *Nature* **2000**, *404*, 59.
- (4) Sun, Y. G.; Xia, Y. N. *Science* **2002**, *298*, 2176–2179.
- (5) Wang, X.; Li, Y. D. *Angew. Chem., Int. Ed.* **2003**, *42*, 3497.
- (6) Wang, X.; Zhuang, J.; Peng, Q.; Li, Y. *Nature* **2005**, *437*, 121.
- (7) Decher, G. *Science* **1997**, *277*, 1232.
- (8) Gao, M.; Richter, B.; Kirstein, S.; Möhwald, H. *J. Phys. Chem. B* **1998**, *102*, 4096.
- (9) Hao, E.; Lian, T. *Langmuir* **2000**, *16*, 7978.
- (10) Malynych, S.; Robuck, H.; Chumanov, G. *Nano Lett.* **2001**, *1*, 647.

- (11) Tripp, S. L.; Pusztay, S. V.; Ribbe, A. E.; Wei, A. *J. Am. Chem. Soc.* **2002**, *124*, 7914.
- (12) Murray, C. B.; Kagan, C. R.; Bawendi, M. G. *Science* **1995**, *270*, 1335.
- (13) Motte, L.; Billoudet, F.; Lacaze, E.; Pileni, M. P. *Adv. Mater.* **1996**, *8*, 1018.
- (14) Springholz, G.; Holy, V.; Pinczolit, M.; Bauer, G. *Science* **1998**, *282*, 734.
- (15) Sun, S.; Murray, C. B.; Weller, D.; Folks, L.; Moser, A. *Science* **2000**, *287*, 1989.
- (16) Talapin, D. V.; Shevchenko, E. V.; Kornowski, A.; Gaponik, N.; Haase, M.; Rogach, A. L.; Weller, H. *Adv. Mater.* **2001**, *13*, 1868.
- (17) Huang, Y.; Duan, X.; Wei, Q.; Lieber, C. M. *Science* **2001**, *291*, 630.
- (18) Redl, F. X.; Cho, K.-S.; Murray, C. B.; Ó'Brien, S. *Nature* **2003**, *423*, 968.
- (19) Fan, H.; Yang, K.; Boye, D. M.; Sigmon, T.; Malloy, K. J.; Xu, H.; Lopez, G. P.; Brinker, C. J. *Science* **2004**, *304*, 567.
- (20) Tang, Z.; Zhang, Z.; Wang, Y.; Glotzer, S. C.; Kotov, N. A. *Science* **2006**, *314*, 274.
- (21) Liu, M.; Xu, G.; Liu, Y.; Chen, Q. *Langmuir* **2001**, *17*, 427.
- (22) Yuan, J.; Liu, M. *J. Am. Chem. Soc.* **2003**, *125*, 5051.
- (23) Huang, X.; Li, C.; Jiang, S.; Wang, X.; Zhang, B.; Liu, M. *J. Am. Chem. Soc.* **2004**, *126*, 1322.
- (24) Mann, S. *Nature* **1988**, *332*, 119.
- (25) Kuzmenko, I.; Buller, R.; Bouwman, W. G.; Kjær, K.; Als-Nielsen, J.; Lahav, M.; Leiserowitz, L. *Science* **1996**, *274*, 2046.
- (26) Cooper, S. J.; Sessions, R. B.; Lubetkin, S. D. *J. Am. Chem. Soc.* **1998**, *120*, 2090.
- (27) Constable, E. C. *Angew. Chem., Int. Ed.* **1991**, *30*, 1450.
- (28) Verbiest, T.; Van elshocht, S.; Kauranen, M.; Hellemans, L.; Snauwaert, J.; Nuckolls, C.; Katz, T.; Persoons, A. *Science* **1998**, *282*, 913.
- (29) Oda, R.; Huc, I.; Schmutz, M.; Candau, S. J.; Mackintosh, F. C. *Nature* **1999**, *399*, 566.
- (30) Meldrum, F. C.; Kotov, N. A.; Fendler, J. H. *J. Phys. Chem.* **1994**, *98*, 4506.
- (31) Lefebure, S.; Ménager, C.; Cabuil, V.; Assenheimer, M.; Gallet, F.; Flament, C. *J. Phys. Chem. B* **1998**, *102*, 2733.
- (32) Liu, M.; Gan, L.; Xu, Z.; Hao, Z.; Chen, G.; Chen, L. *Colloids Surf., A* **2007**, *301*, 432.
- (33) Liu, M.; Gan, L.; Zeng, Y.; Wang, J.; Xu, Z.; Hao, Z.; Chen, G.; Liu, H.; Chen, L. *Chem. Lett.* **2007**, *36*, 308.
- (34) Kang, Y. S.; Risbud, S.; Rabolt, J. F.; Stroeve, P. *Chem. Mater.* **1996**, *8*, 2209.
- (35) Kang, Y. S.; Risbud, S.; Rabolt, J. F.; Stroeve, P. *Langmuir* **1996**, *12*, 4345.
- (36) Lee, D. K.; Kang, Y. S.; Lee, C. S.; Stroeve, P. *J. Phys. Chem. B* **2002**, *106*, 7267.
- (37) Jiang, M.; Zhai, X.; Liu, M. *Langmuir* **2005**, *21*, 11128.
- (38) Menger, F. M.; Littau, C. A. *J. Am. Chem. Soc.* **1993**, *115*, 10083.
- (39) Oda, R.; Huc, I.; Schmutz, M.; Candau, S. J.; MacKintosh, F. C. *Nature* **1999**, *399*, 566.
- (40) In, M.; Bec, V.; Aguerre-Chariol, O.; Zana, R. *Langmuir* **2000**, *16*, 141.
- (41) Zhai, X.; Zhang, L.; Liu, M. *J. Phys. Chem. B* **2004**, *108*, 7180.
- (42) Zhou, M.; Liu, H. L.; Yang, H. F.; Liu, X. L.; Zhang, Z. R.; Hu, Y. *Langmuir* **2006**, *22*, 10877.
- (43) Li, L.; Qian, H.; Fang, N.; Ren, J. *J. Lumin.* **2006**, *116*, 59.
- (44) McConnell, H.; Moy, V. *J. Phys. Chem.* **1988**, *92*, 4520.
- (45) Vollhardt, D.; Melzer, V. *J. Phys. Chem. B* **1997**, *101*, 3370.
- (46) Teer, E.; Knobler, C.; Lautz, C.; Wurlitzer, S.; Kildae, J.; Fischer, T. *J. Chem. Phys.* **1997**, *106*, 1913.
- (47) Liu, M.; Gan, L.; Hao, Z.; Xu, Z.; Zhu, D.; Chen, L. *Chin. J. Chem.* **2008**, *26*, 39.